Celerity and magnitude of pressure surges in rectangular section pipes and conduits

A.T. Sayers[1] and **H.L. van Zyl**[2]

(First received November 1993; Final version March 1994)

Abstract

Rectangular section pipes are being increasingly used by industry. This paper describes the determination of the celerity and magnitude of pressure surges in rectangular cross-section steel and aluminium pipes for the long side to wall thickness ratio $9 < \frac{x}{t} < 30$. *The results are compared with analytical equations for the celerity which take account of pipe wall shear, bending, tension and Poisson's ratio. The wave celerity decreases the more the pipe cross-sectional area departs from square.*

Nomenclature

A	mean cross-sectional area of pipe (xy), m^2
c	celerity of pressure surge relative to undisturbed fluid, m/s
E	modulus of elasticity of the pipe material, Pa
G	shear modulus of pipe material, Pa
K	bulk modulus of elasticity of the liquid, Pa
l	mean length of side of square section pipe, m
T	measured time for wave travel, s
t	thickness of pipe wall, m
V	steady state flow velocity, m/s
v	celerity of pressure surge relative to stationary pipe, m/s
x	mean length of long side of rectangular pipe, m
y	mean length of short side of rectangular pipe, m
ρ	density of liquid, kg/m^3
ν	Poisson's ratio
ϕ	a function of
ΔA	change in cross-sectional area, m^2
Δp	magnitude of pressure surge, N/m^2
ΔV	mean decrease in steady state flow velocity during surge, m/s

Subscripts

bs	due to bending and shear
t	due to wall stretch

Introduction

Prediction of the celerity and magnitude of pressure surges in circular section pipes and conduits is well established, and there exists a large body of experimental data to support the theoretical equations upon which those predictions are based. In recent years, pipelines of rectangular cross-section have been increasingly used in power station cooling water systems, aircraft fuel systems and aerospace applications. It is therefore not surprising that attention has been geven to the prediction of the surge magnitude and celerity in such conduits. However, the theoretical equations emanating from such studies have not been correlated, to any significant degree, with experimental data.

Hill [1] developed equations for the celerity of a pressure surge in rectangular section pipes using simple steady state theory to describe the deformation of the pipe walls under the increased surge pressure. Each side-wall of the pipe was considered to be an encastre beam which deformed due to the action of a uniformly distributed load, the corners of the pipe remaining at fixed points in space and undergoing no rotation, while pipe wall inertia and end effects due to longitudinal restraint were neglected.

Jenkner's [2] analysis of thin walled rectangular pipes allowed for rotation of the pipe wall corners with no restriction on them being fixed in space, thus allowing him to take account of stretching of the side-walls as well as bending deflections. For a thin walled square section pipe, ($\frac{l}{t} > 20$), Jenkner derived an identical equation to that of Hill and he therefore concluded that the effect of pipe wall stretch has a negligible effect on the transient velocity occurring during surge.

Thorley & Guymer [3] extended the work of Hill to include the effects of shear forces on the deflection of the side-walls of the pipe, and lateral stretch of the walls. Effects due to bending about a longitudinal axis in the pipe walls, and pipe wall inertia were neglected, and no account was taken of the influence of longitudinal pipe restraint and the subsequent influence of Poisson's ratio. These authors also presented three experimental data points for pipe flow velocities in the range 0.195 to 0.339 m/s in aluminium and steel pipes of various cross-sections. These differed by between 6.5 and 16.8 % from their theoretical predictions. Thorley & Guymer also calculated the expected pressure change using the Joukowski relationship ($\Delta p = \rho c \Delta V$) and concluded that it was within 2 % of the experimentally observed pressure.

Sayers [4] further extended the work of Thorley & Guymer to include the effect of Poisson's ratio on the stretch of the pipe walls. Experimental pressure surge celerities were determined for square section steel pipes in the range $12.9 < (\frac{l}{t}) < 27.2$ and these were within 8% of the theoretical predictions. This paper extends the

[1]Associate Professor, Department of Mechanical Engineering, University of Cape Town, Private Bag, Rondebosch, 7700 Republic of South Africa (Member)

[2]Graduate, University of Cape Town

work of Sayers to rectangular section pipes, and shows that the developed analytical equations may be used with confidence.

Governing equations

Figure 1 shows a stretch δz of a rectangular cross-section pipe having mean side length of x and y. If a pressure surge of magnitude Δp above the steady state pressure takes place, the celerity c of the transient pressure wave relative to the fluid into which it is moving, is given by [5]

$$c = \left\{ \rho \left[\frac{l}{K} + \frac{\left(\frac{\Delta A}{\Delta p}\right)}{A} \right] \right\}^{-\frac{1}{2}} \tag{1}$$

and depends on the variable $(\frac{\Delta A}{\Delta p})$ for its magnitude. Therefore the method of evaluation of $(\frac{\Delta A}{\Delta p})$ is very important. Three parameters contributing to the change in cross-section of a rectangular pipe section were considered by Thorley & Guymer.[3] These were:

1. side-wall deflection due to bending moments resulting from an internal pressure change;
2. shear forces acting in the pipe walls;
3. stretching of the sides of the pipe walls due to the internal pressure change.

These parameters each contributed to ΔA to give

$$\Delta A = \Delta A_{bs} + \Delta A_t$$

where ΔA_{bs} is the combined area change due to bending and shear, while ΔA_t is the flow cross-sectional area change caused by pipe wall stretch. ΔA_{bs} was found to be given by [3]

$$\Delta A_{bs} = \Delta p \frac{\left\{ \frac{(x^3+y^3)\left(\frac{x^3}{6}+\frac{x^2y}{2}-\frac{y^3}{3}\right)}{2(x+y)} - \frac{x^5}{20} - \frac{x^2y^3}{4} + \frac{y^5}{5} + \frac{Et^2(x^3+y^3)}{4G} \right\}}{t^3E} \tag{2}$$

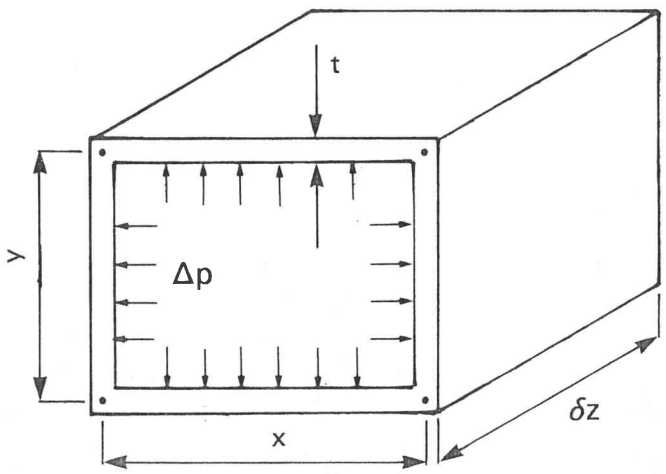

Figure 1 Rectangular section pipe element.

Putting

$$\frac{\left(\frac{\Delta A_{bs}}{\Delta p}\right)}{A} = \frac{\phi_{bs}(x,y)}{xyt^3E} \tag{3}$$

where $\phi_t(x,y)$ is the function within the curly brackets of equation (2), then

$$\frac{\left(\frac{\Delta A}{\Delta p}\right)}{A} = \frac{[\phi_{bs}(x,y) + \phi_t(x,y)]}{xyt^3E} \tag{4}$$

where $\phi_t(x,y)$ is the function due to the stretching of the pipe walls.

Thorley & Guymer [3] assumed that the tensile forces in the pipe walls were given by $\frac{\Delta p x \delta z}{2}$ and $\frac{\Delta p y \delta z}{2}$, respectively, while Sayers [4] introduced the influence of the method of pipe support into the analysis for $\phi_t(x,y)$. Sayers considered three methods of longitudinal pipe support:

1. pipe ends are free to move longitudinally so that there is no longitudinal stress in the pipe walls;
2. pipe ends are rigidly clamped to prevent longitudinal strain in the pipe walls;
3. restraint where there exists both longitudinal stress and longitudinal strain in the pipe walls.

Table 1 $\phi_t(x,y)$ for three cases of longitudinal pipe restraint

Case	$\phi_t(x,y)$
(a)	$\frac{xyt^2(x+y)(1-\nu)}{2}$
(b)	$\frac{xyt^2(x+y)(1-\nu-2\nu^2)}{2}$
(c)	$\frac{xyt^2(x+y)\left(1-\nu\left[1+\frac{xy}{(x+y)^2}\right]\right)}{2}$

The resulting functions for $\phi_t(x,y)$ are shown in Table 1 where the stretch of the pipe wall is modified by the inclusion of Poisson's ratio for the pipe material. Equation (1) can therefore be written as

$$c = \left\{ \rho \left[\frac{1}{K} + \frac{\phi(x,y)}{xyt^3E} \right] \right\}^{-\frac{1}{2}} \tag{5}$$

where $\phi(x,y) = [\phi_{bs}(x,y) + \phi_t(x,y)]$.

Experimental apparatus

The experimental test rig is shown in Figure 2. The rectangular pipe test sections consisted of commercially available hot rolled mild steel pipes and aluminium extrusions. The steel pipes were divided into two sets, the pipes comprising a set having approximately the same nominal outside dimensions, but differing wall thickness. The aluminium pipes had a wider variation in their dimensions. A number of measurements, to within 0.01 mm, were taken of the outside dimensions and wall thickness of each pipe. These were averaged and are tabulated in Table 2. The fillet radii of the pipes were of the same order of magnitude as the wall thickness.

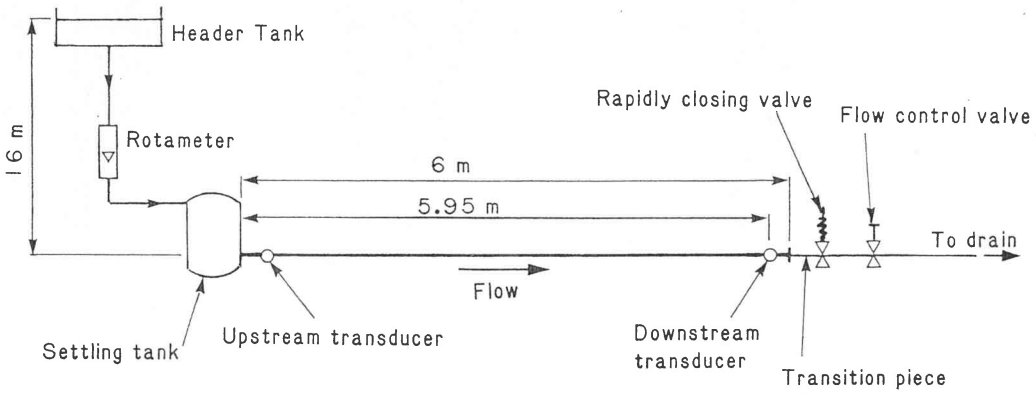

Figure 2 Experimental test rig.

Table 2 Averaged dimensions of the test sections

Pipe No. and material	Outer dimensions and wall thickness (mm)	x (mm)	y (mm)	x/y	x/t
1 MS	31.58 × 19.31 × 1.70	29.88	17.61	1.70	17.60
2 MS	31.57 × 18.85 × 2.15	29.42	16.70	1.76	13.68
3 MS	31.39 × 18.94 × 2.53	28.86	16.41	1.76	11.40
4 MS	31.85 × 20.06 × 3.00	28.85	17.06	1.69	9.61
5 MS	38.05 × 18.98 × 1.74	36.31	17.24	2.11	20.86
6 MS	37.97 × 19.93 × 2.05	35.92	17.88	2.01	17.52
7 MS	38.37 × 18.99 × 2.50	35.87	16.49	2.18	14.30
8 MS	40.12 × 19.75 × 3.12	37.00	16.63	2.22	11.86
9 AL	33.10 × 20.40 × 1.07	32.03	19.33	1.66	29.93
10 AL	32.97 × 20.17 × 1.58	31.39	18.59	1.69	19.86
11 AL	39.62 × 20.51 × 1.52	38.10	18.99	2.01	25.10

The pipes were 6 m long with two transducer pockets welded onto the outer wall at 50 mm from each end, and into which were screwed two 25 mm diameter inductance pressure transducers. The pockets were provided with air bleed holes for the release of any entrapped air prior to surge. Each Transducer pocket was connected to the fluid in the pipe via a 4 mm diameter hole 9 mm long, drilled through the pocket and pipe wall. Similar pockets had been used in similar experiments on circular pipes and had been found to give excellent results. The upstream end of the pipe was connected, via a flange, to a settling tank which was supplied with water from a 16 m high constant head tank through a rotameter used for measurement of the water flow rate. The rotameter was calibrated by weighing water collected over a period of time to generate a linear calibration curve. The error bound on the measurement of flow rate was ± 1 %. Each pipe was clamped at intervals of 650 mm along its length to prevent longitudinal expansion (i.e. case (b) of Table 1), and also to reduce longitudinal and lateral vibration.

A rapidly closing valve placed at the downstream end of the pipe had an orifice diameter of 20 mm. To achieve a smooth flow transition from the rectangular pipe section to a circular section, a rectangular-to-round tapering transition piece 200 mm long was made to suit each pipe. This was inserted between the downstream end of the pipe and the rapidly closing valve.

The fast action solenoid-operated valve was closed in 5.6 milliseconds under the action of a helical spring possessing a stiffness of 32.2 N/mm. The closure time was of sufficiently short duration to be regarded as rapid, according to the criterion that for all runs the valve was fully closed before the return of the pressure wave reflected from the upstream reservoir. The pressure surge was detected by the two transducers whose signals were amplified and displayed on a storage oscilloscope screen which was triggered during steady state flow before activation of the solenoid. From these recordings for different flow rates through each pipe, the celerity of the pressure surge and its magnitude were measured. Although the pressure at the upstream transducer was recorded, it was not needed to determine the wave celerity but was used as a check on the celerity determined from the downstream transducer.

Results

For a steel pipe of 20 mm short side-wall length, equation (5) case (b) [hereinafter called equation (5b)] is plotted against wall thickness in Figure 3 for three different long side-wall lengths. In Figure 4, equation (5b) is plotted for a given pipe size (40 × 20 mm) for aluminium and steel. Figure 5 shows a typical recorded downstream transducer pressure surge trace. The distance T represents the time taken for the surge wave to travel from the downstream

transducer to the upstream reservoir, and then back to the downstream transducer as a reflected cancelling wave. The point at which the pipe pressure begins to rise above the steady state pressure is taken as the time when the surge wave due to sudden valve closure first reaches the down stream transducer, while the point at which the surge pressure suddenly falls is taken at the time of arrival of the reflected wave back at the downstream transducer. Therefore since the distance from the downstream transducer to the reservoir is 5.95 m, the wave celerity relative to the stationary pipe is given by

$$v = \frac{11.9}{T} \tag{6}$$

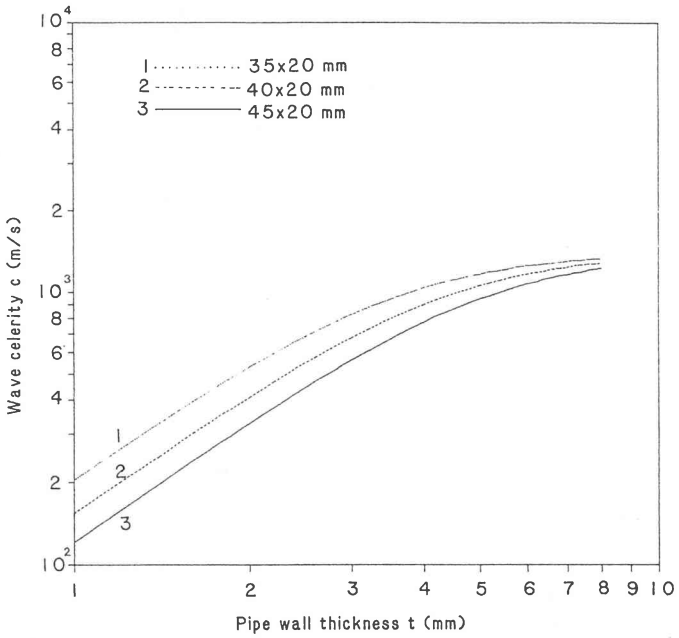

Figure 3 Variation of wave celerity with pipe wall thickness for steel pipes of fixed short side length from equation (5b). ($y = 20$ mm, $E = 200$ GPa, $G = 82.7$ GPa, $\nu = 0.3$, $K_{\text{water}} = 2.05$ GPa).

If the reduction in steady state flow velocity ΔV is negligible when compare with v, then c may be assumed to be approximately equal to v. In these experiments ΔV is little more than 1 % of v, hence the mean celerity c for the range of water flow rates for each pipe was determined, and is compared with the theoretical celerity calculated from equation (5b), in Table 3.

In Table 2 the steel pipes are split into two basic groups comprising pipes 1–4 and 5–8, respectively, in which the side lengths are approximately constant within each group, while for both groups the average length of the shorter side is the same. The average pipe sizes were (31.6 × 19.3 mm) and (38.6 × 19.4 mm), respectively, and inserting these lengths into equation (5b), the theoretical celerity was calculated and plotted in Figure 6 as a function of pipe wall thickness. The appropriate experimentally determined celerities for each pipe in a set are also plotted in Figure 6.

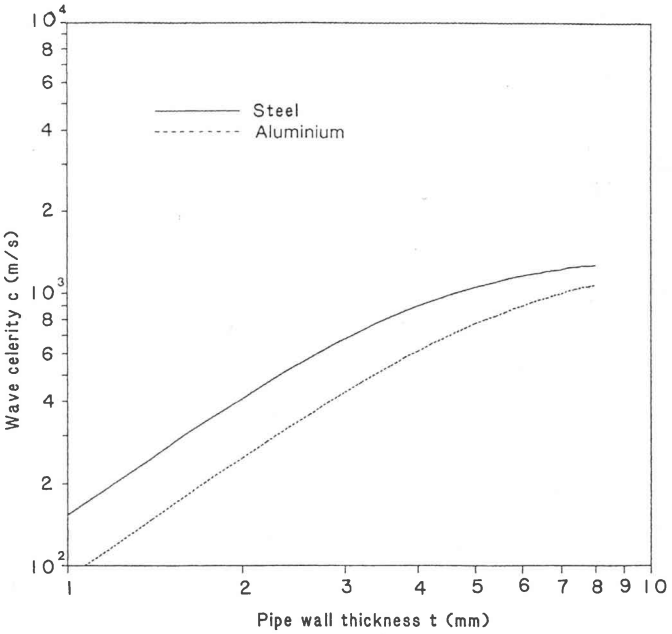

Figure 4 Wave celerity vs. wall thickness from equation (5b) for the aluminium and steel pipes. ($x = 40$ mm, $y = 20$ mm).
For steel: $E = 200$ GPa, $G = 82.7$ GPa, $\nu = 0.3$.
For aluminium: $E = 69$ GPa, $G = 27.6$ GPa, $\nu = 0.33$.
For water: $K = 2.05$ GPa.

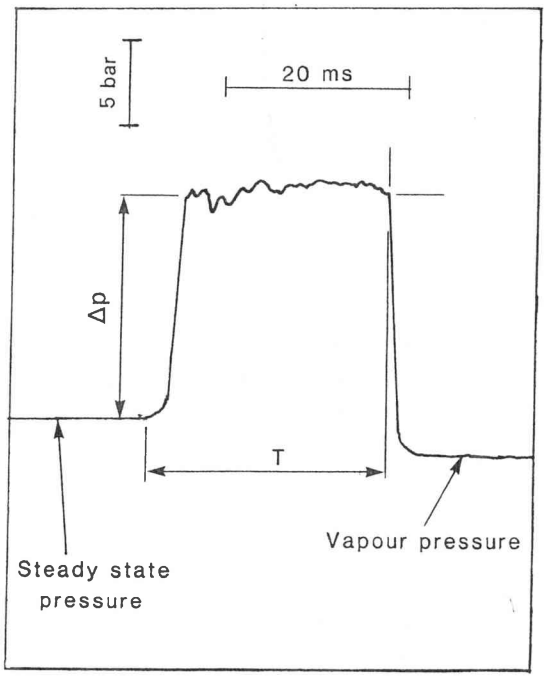

Figure 5 Typical pressure surge recording.

Referring again to Figure 5, the surge pressure was taken at the height reached by the initial surge. Although some perturbations above and below this pressure, caused by extraneous vebrations or the presence of small vapour cavities were observed, the mean surge pressure during the

wave travel was in general easily defined. The experimental surge pressures measured at each flow rate are compared in Figure 7 with those calculated from the Joukowski surge pressure relationship of equation (7).[5]

$$\Delta p = \rho c \Delta v \tag{7}$$

When calculating Δp using equation (7), the experimentally determined values of c and Δv were used. Equation (7) can also be expressed in dimensionless form as a pressure surge coefficient $\left(\frac{\Delta p}{\rho \Delta v^2}\right) = \phi\left(\frac{c}{\Delta v}\right)$ and this functional relationship is plotted in Figure 8 for the measured surge pressures and velocities.

Table 3 Comparison between theoretical and experimental celerity of a pressure surge for rectangular section steel and aluminium pipes

$E_{\text{steel}} = 200$ GPa, $G = 82.7$ GPa, $\nu = 0.3$

$E_{\text{alum.}} = 69$ GPa, $G = 27.6$ GPa, $\nu = 0.33$

$K_{\text{water}} = 2.05$ GPa

Pipe No.	Mean celerity: Equation (5b)	c (m/s) Experiment	% difference
1 MS	535.3	531.3	−0.75
2 MS	702.9	683.6	−2.75
3 MS	843.7	819.8	−2.84
4 MS	984.0	947.5	−3.71
5 MS	377.4	373.0	−1.15
6 MS	488.5	487.2	−0.26
7 MS	601.9	595.1	−1.13
8 MS	737.7	700.4	−5.05
9 AL	156.7	163.3	+4.21
10 AL	278.9	279.2	+0.11
11 AL	179.0	186.6	+4.24

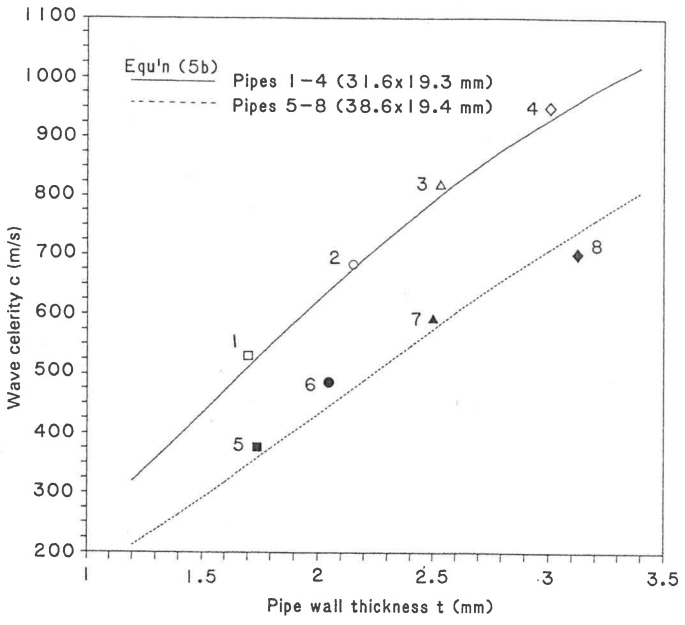

Figure 6 Experimental celerity vs. pipe wall thickness for steel pipes. (Pipe number attached to symbol).

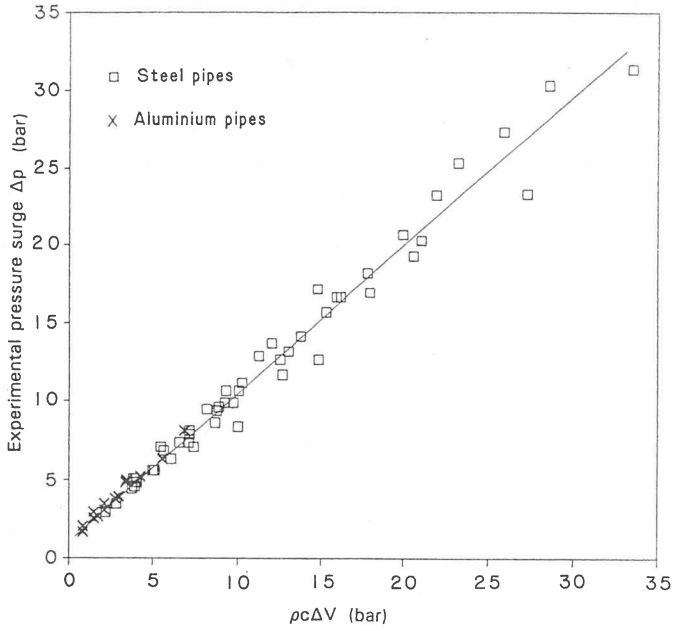

Figure 7 Experimental surge pressure vs. Joukowski surge pressure (equation 7).

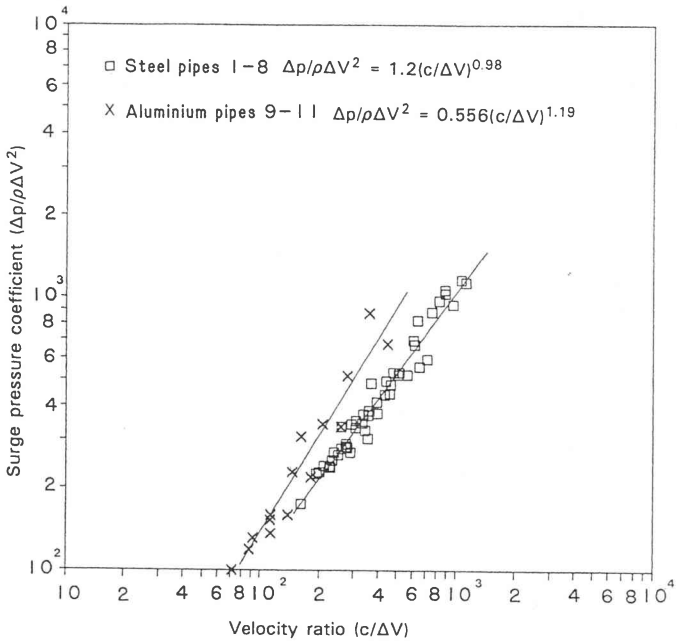

Figure 8 Surge pressure coefficient vs. velocity ratio for steel and aluminium pipes.

Discussion

In Figure 3, for a given constant pipe size, equation (5b) shows an increase in wave celerity with wall thickness which gives good correlation to a logarithmic function of the form $\log(c) = (a)\log(t)$ over the range $1 < t < 3$. This range of wall thickness is that most likely to be found in commercial practice. At greater wall thicknesses the celerity departs from the simple logarithmic form, and tends

towards the speed of sound in an infinitely large expanse of fluid, since $\frac{\Delta A}{A}$ in equation (1) then tends towards zero. The sensitivity of the celerity to changes in the length of the long side-wall for a given wall thickness is greatest at small wall thickness. In particular, at a 2 mm wall thickness the celerity decreases by approximately 38 % for a 29 % increase in long side-wall length.

Sensitivity of the wave celerity to changes in pipe material is illustrated in Figure 4 where, for the aluminium pipe, the combinations of lower moduli of elasticity and shear coupled with a higher Poisson's ratio causes a substantial reduction in wave celerity.

Table 3 shows excellent agreement between the experimental and theoretical results, the average difference being in the order of 2 %. Thorley & Guymer [3] reported a 16.8 % difference between the observed and theoretical celerity when ignoring the effect of Poisson's ratio. The slight differences in the nominal side-wall length of the pipes used in the experiments do not seriously affect the calculated celerity. This is proved in Figure 6 where the experimental wave celerities are compared with theoretical curves from equation (5b) drawn for the averaged nominal side-wall lengths. As the cross-section of the pipe departs from a square, so the wave celerity decreases. For pipes 1–4, the ratio $\frac{x}{t}$ at a wall thickness of 2 mm is 15.8, while the corresponding celerity is 620 m/s. For a similar $\frac{x}{t}$ in a square pipe, Sayers [4] reported a celerity of 750 m/s.

The measured surge magnitude (Figure 7) agrees, to within 2.5 %, with that calculated from the measured wave celerity and steady state velocity using the standard Joukowski relationship of equation (7). Thus the magnitude of the pressure surge is independent of the pipe size, cross-section, material and method of constraint, and depends only on the wave celerity for a given ΔV. In Figure 8 the surge pressure coefficients for each pipe material fall into two distinct bands with the best fit power laws defined in the figure. For other pipe materials, similar power laws will be obtained.

Conclusions

The celerity and magnitude of pressure surges in rectangular section steel and aluminium pipes have been experimentally measured for a range of steady state flow velocities. These have been compared with theoretically determined values obtained from an equation which includes the effects of pipe wall shear and tensile stresses, pipe wall deflections due to bending moments, and the influence of Poisson's ratio. Excellent agreement between experiment and theory was found to occur.

The celerity of the pressure decreases the more the pipe cross-section departs from square, while for $\frac{x}{t} > 10$ the variation of celerity is approximately linear on a log-log scale.

The surge magnitude follows the Joukowski relationship. Pressure coefficients embodying the wave celerity and surge magnitude have been defined, empirical relationships for the surge pressure coefficients for rectangular steel and aluminium pipes are presented.

The analytical equations for the surge celerity may be used with confidence.

References

[1] Hill DJ. Fluid transients in pipes of non-circular cross-section. *Final Year Project Report No. 385*, 1970, The City University, London.

[2] Jenkner WR. Uber die Druckstossgeschwindigkeit in Rohrleitungen mit quadratischen un rechteckigen Querschnitten. *Schweizerische Bauzeiting*, 1971, **89**(5), 99–103.

[3] Thorley ARD & Guymer C. Fundamental equations governing pressure surge phenomena in pipes of rectangular cross-section. *Proc. Instn. Mech. Engrs.*, 1975, **189**, 325–332.

[4] Sayers AT. Poisson's ratio effects on the celerity of a pressure surge in rectangular section pipes. *ASME fluid transients in fluid-structure interaction*, Miami 1985, 109–114.

[5] Massey BS. *Mechanics of Fluids*, 5th edn. Van Nostrand Reinhold, 1983.